JOURNAL OF THE KOREAN ASTRONOMICAL SOCIETY
38: 471 ~ 478, 2005

STRATOSPHERIC IMAGES OF JUPITER DERIVED FROM HYDROCARBON EMISSIONS IN VOYAGER 1 AND 2 IRIS SPECTRA

HAINGJA SEO[1], SANG JOON KIM[1], W. K. CHOI[2], T. KOSTIUK[3], AND G. BJORAKER[3],
[1]Department of Astronomy & Space Science, Kyung Hee University, Suwon, 449-701, Korea
E-mail: sjkim1@khu.ac.kr
[2] School of Earth and Environmental Sciences Seoul National University, Seoul, 151-747, Korea
[3] NASA/GSFC, Greenbelt, MD 20771, USA
(Received November 21, 2005; Accepted December December 5, 2005)

ABSTRACT

Spectroscopic data obtained by the Infrared Interferometer Spectrometer (IRIS) aboard Voyager 1 and 2 have been re-visited. Using the spectroscopic data and footprints of the IRIS aperture on the planet, we constructed images of the stratosphere of Jupiter at the emission bands of hydrocarbons including CH_4, C_2H_6, C_2H_2, C_3H_4, C_6H_6, and C_2H_4. Thermal emission from the hydrocarbons on Jupiter originates from a broad region of the stratosphere extending from 1 to 10 millibars. We averaged the data using a bin of 20 degrees of longitude and latitudes in order to increase signal-to-noise ratios. The resultant images show interesting wave structure in Jupiter's stratosphere. Fourier transform analyses of these images yield wavenumbers 5 - 7 at mid-Northern and mid-Southern latitudes, and these results are different from those resulted from previous ground-based observations and recent Cassini CIRS, suggesting temporal variations on the stratospheric infrared pattern. The comparisons of the Voyager 1 and 2 spectra also show evidence of temporal intensity variations not only on the infrared hydrocarbon polar brightenings of hydrocarbon emissions but also on the stratospheric infrared structure in the temperate regions of Jupiter over the 4 month period between the two Voyager encounters. Short running title: Stratospheric Images of Jupiter derived from Voyager IRIS Spectra.

Key words : Jupiter, atmosphere, stratosphere, infrared, molecules

I. INTRODUCTION

The IRIS on Voyager 1 and 2 (Hanel et al. 1979a, b) harvested a wealth of information on the atmospheres of the outer planets. The IRIS infrared spectra have been used to study the thermal structures (e.g., Conrath and Gautier, 1980), gas mixing ratios (e.g., Kunde et al. 1982), ammonia cloud layers (e.g., Marten et al. 1981), and dynamics (e.g., Gierasch et al. 1986) of Jupiter. These studies used primarily Voyager 1 data because Voyager 2 data are noisier in the shorter wavelength range compared with Voyager 1 data. Analyzing the Voyager IRIS spectra, detections of tropospheric waves were reported by Deming et al. (1989) and Magalhães et al. (1989); and stratospheric features were observed at NASA/IRTF (Infrared Telescope Facility) by Orton et al. (1991). However, stratospheric features made from the Voyager IRIS data have not been reported thus far. The NIMS (Near Infrared Mapping Spectrometer) on Galileo covered the 0.7 ~ 5.2 μm range, and could not observe the thermal infrared range (7.14 - 50 μm) that the IRIS on Voyager 1 and 2 covered.

In this paper, we constructed stratospheric images using selected spectral regions of the Voyager IRIS data. We averaged the Voyager data using a bin of 20 degrees of longitude and latitudes in order to increase signal-to-noise ratios. Global stratospheric images of Jupiter were constructed at the central emission bands of major hydrocarbons, such as, CH_4, C_2H_6, and C_2H_2. The constructed images revealed patterns of wave-like stratospheric structure. Although Voyager 1 data were primarily utilized, we also analyzed Voyager 2 data, which have not been fully evaluated to study the stratosphere.

Recently, the Cassini Composite Infrared Spectrometer (CIRS) obtained thermal infrared spectra of Jupiter with a spectral resolution of 0.003 μm and spatial resolutions of approximately 3° covering the entire globe (e.g., Flasar et al. 2001; Achterberg et al. 2001). Using the CIRS spectra, Achterberg et al. (2001) constructed global images for the stratosphere and the troposphere, and found that the images are dominated by zonal wavenumber 2 along with other wavenumbers at various latitudes. Harrington et al. (2001) observed Jupiter at the NASA/IRTF with the MIRLIN camera, and reported the stratospheric waves with zonal wavenumber 1 and 13 at 18° south.

We discuss the patterns of the stratospheric waves shown on our IRIS images, and compare the features with other wave-like features reported previously by other authors. We also made one-dimensional longitudinal images of the polar regions for these hydrocarbons, and minor species, such as C_3H_4, C_6H_6, and C_2H_4, which appear only in the auroral IRIS spectra

Corresponding Author: S. J. Kim

(Kim et al. 1985). We compare Voyager 1 and 2 polar spectra in order to investigate temporal variations of infrared auroral emissions and stratospheric infrared structure between the two Voyager Jupiter encounters.

II. DATA REDUCTION

The IRIS aboard Voyager 1 and 2 acquired infrared spectra of Jupiter covering nearly all Jupiter's surface from 7.14 μm to 50μm (Figs. 1a and 1b). Observational sequences known as North/South maps were performed as each spacecraft approached and receded from Jupiter. These maps have 360° of longitude coverage of Jupiter. We selected data obtained from a time span of 6 days before and after the closest encounters, which correspond to FDSC (Flight Data System Count) 16209.24 - 16569.24 for Voyager 1, and FDSC 20479.30 - 20839.30 for Voyager 2. We carefully selected and averaged these data in order to increase signal-to-noise (S/N) ratios.

We first calculated realistic IRIS aperture shapes projected onto the Jupiter's surface. If the aperture shape is too elongated, ie., if the radius is greater than 15° from the centers of the apertures, then this area is discarded. We averaged overlapping regions of two or more of apertures. Figures 1a and 1b show the resultant footprints of the Voyager 1 and 2 IRIS apertures, respectively, on the surface of Jupiter for the C_2H_2 emissions. As shown in these figures, there are some missing regions, colored by black. As noted immediately, these images in Figures 1a and 1b are too noisy to discern any stratospheric structure of the C_2H_2 emissions except the bright north polar auroral region. Therefore, we decided to bin the images with larger longitude and latitude intervals compared with the sizes of the apertures in order to increase S/N ratios, as follows:

We have developed procedures to average the data in bins whose widths are 20° of longitude and latitude. As seen in Figures 1a and 1b, most of the aperture sizes are smaller than the 20° × 20° bin. The radiances of Jupiter at frequencies corresponding to emission bands of hydrocarbons or to the pressure-induced absorptions (PIA) of molecular hydrogen were extracted from the IRIS spectra. The spectral radiances within the bin were then averaged together to improve S/N ratios. A point is plotted every 4° longitude and every 5° latitude except high latitudinal regions. The pixel size in the resultant images are, therefore, 4° longitude and 5° latitude for the region between -45° and +45° latitude. For the polar regions, we used wider latitudinal bins: 50° - 90°, and 50° 90°S latitudes considering the sparsity of the polar data. In the high latitudinal regions, the number of spectra are scarce as seen in Figures 1a and 1b, except a north polar region near 60° N and 180° System III longitude. Bins with only 1 or 2 spectra have the largest error bars while bins with best S/N ratios have 75 or more spectra.

The $\pm 1\sigma$ error bar for a radiance corresponding a bin has been calculated using the following equation:

$$1\ \sigma\ \text{S/N ratio} = \frac{NESR}{\sqrt{N}}, \qquad (1)$$

where $NESR$ is the noise equivalent spectra radiance taken from Hanel et al. (1980), and N is the number of spectra in a bin.

The averaged and binned data of the FDSC 16209.24 - 16569.24 for Voyager 1, and FDSC 20479.30 - 20839.30 for Voyager 2 are presented in Figures 2 through 7. However, these data cover a time span of more than 10 days, and there might be temporal variations of the stratospheric infrared emissions during this period especially due to stratospheric winds (e.g., Conrath et al. 1990). In order to see any variations of the infrared emissions during this period, we selected a data set out of the IRIS data which were taken on 2 - 3 days before (FDSC 16308.40 - 16326.39) the closest encounter with Jupiter. These Voyager 1 data cover the entire globe and the S/N ratio for each data point is sufficient to make global maps, which are presented in Figure 8.

In order to study molecular emissions from the stratosphere of Jupiter, one must carefully subtract the underlying tropospheric continuum. Stratospheric emission lines of most hydrocarbon molecules are formed approximately at the 1 - 10 mbar pressure levels, while the PIA of molecular hydrogen at the same frequencies originate from the 400 - 500 mbar levels. Although one could subtract the continuum from a particular emission at nearby frequency, this may introduce significant noise when the underlying continuum has a low S/N ratio. Instead we chose a different frequency where unit optical depth of the PIA of molecular hydrogen occurs at the same pressure level but where the S/N is much higher. For example, C_2H_2 emission at 13.66 μm is riding on a 124 K molecular hydrogen continuum. The absorption coefficient of the PIA of molecular hydrogen is the same at 31.25 μm and 13.66 μm, but the radiance from a 124 K black body is 10 times higher at 31.25 μm than at 13.66 μm. Thus, one can use the molecular hydrogen continuum at frequencies where both Voyager 1 and 2 have good S/N, to remove tropospheric temperature effects approximately. As seen in Figure 2 through Figure 5, which show longitudinal variation of the hydrocarbon emissions, the resultant S/N ratios derived from the above procedures are meaningful to study the infrared images of the polar regions of Jupiter.

III. INFRARED POLAR EMISSIONS

Although the high latitudinal regions have been scarcely observed by Voyagers, a north polar region (near 60° N and 180° System III longitude) was intensely observed by observational sequences, which were programmed by the Voyager team in advance in order to determine the gas composition at the polar regions. This is serendipitous because this particular longitude was not known to have enhanced infrared emission at the times of the Voyager encounters. The north

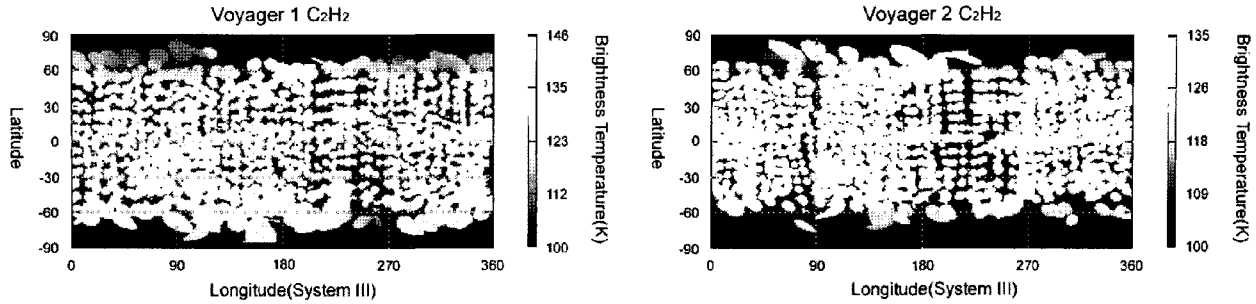

Fig. 1.— Voyager 1 (Fig. 1a) and 2 (Fig. 1b) IRIS field of views projected onto the Jupiter's surface for C_2H_2 emissions during a time span between 6 days before and after the closest encounters, which correspond to FDSC (Flight Data System Count) 16209.24 - 16569.24 for Voyager 1, and FDSC 20479.30 - 20839.30 for Voyager 2. Missing regions are colored by black. The images are too noisy to discern any stratospheric structure of the C_2H_2 emissions except the north polar auroral region. We, therefore, binned the images with larger longitude and latitude intervals than the aperture size in order to increase signal-to-noise ratios, and presented the resultant images in Figs. 6, 7, and 8.

polar hot spot was first detected with ground telescopes in the early 1980s by Caldwell et al. (1980 and 1983). Subsequent careful examinations of the north polar spectra of Voyager 1 IRIS revealed enhanced emissions of several hydrocarbons, such as C_2H_4, C_3H_4, C_6H_6, and possibly CH_3 (Kim et al. 1985). Recently, the Infrared Space Observatory (ISO) observed C_3H_4 and C_4H_2 on Saturn; C_6H_6 on Jupiter and Saturn; and CH_3 on Saturn and Neptune (e.g., Bezard et al., 1999).

Shown in Figure 2 are comparisons of binned intensities between Voyager 1 and 2 data for CH_4, C_2H_6, and C_2H_2 band emissions from the north polar stratosphere. The 6 figure panels show average radiances (i.e., brightness temperatures) and $\pm 1\sigma$ error bars at the selected frequencies corresponding to the band centers of CH_4, C_2H_6, and C_2H_2. Figure 2 clearly shows similar enhanced emissions of CH_4 and C_2H_2 above the noise levels between 160° and 200° longitude for the both Voyager data, except the Voyager 2 C_2H_6 emission, which is prominent compared with that in the Voyager 1 data. This demonstrates the variability of the C_2H_6 emission within a 4 month scale, and the causes are not known at this time.

Figure panels in Figure 3 exhibits detailed longitudinal variations for the band emissions of minor species, C_2H_4, C_3H_4, and C_6H_6 from the north polar regions observed by Voyager 1 and 2. As seen from the upper most figure panel in Figure 3, Voyager 1 data show an enhancement of C_2H_4 emission between 160° - 210° longitude, and probably the feature is wider in longitude than that of the CH4 emission of Voyager 1 in Figure 2. Voyager 2 north polar data (the 2nd figure panel in Fig. 3) are very noisy showing no visible enhancement of C_2H_4 emission around 180°, where we see definite but similar patterns of CH_4, C_2H_6, and C_2H_2 emission enhancements in Voyager 1 data (Fig. 2). Voyager 1 C_3H_4 emission (the 3rd panel of Fig. 3) is weak but perhaps wider (i.e., 140o - 240° longitude) than Voyager 2 C_3H_4 (4th panel) and Voyager 1, 2 C_6H_6 (5th, 6th panels) emissions, which are approximately confined between 160° and 200° longitude. The 4th and 6th panels (Voyager 2 data) show similar emission shapes for C_6H_6 and C_3H_4, but the noise is higher than Voyager 1 C_6H_6 (5th panel).

Figures 4 and 5 show Voyager 1 and 2 south polar data. The 3rd and 5th figure panels in Figure 4 (Voyager 1 data) show C_2H_6 and C_2H_2 emission enhancements between 50° and 110°, and the emission enhancements probably also occur for Voyager 1 C_3H_4 emission (3rd panel, Fig. 5) in the same longitude range. But no similar enhancement can be seen for other Voyager 1 hydrocarbon emissions. The Voyager 2 CH_4 emissions (2nd panel, Fig. 4) are very noisy and do not show any significant longitudinal information.

Voyager 2 south polar data show C_2H_2 emission enhancement approximately between 190° and 270° longitude (6th panel, Fig. 4) and probably C_2H_6 (4th panel, Fig. 4) and C_3H_4 emissions(4th panel, Fig. 5). For the same longitudinal range of the Voyager 2 south polar data, however, we cannot see any visible enhancements for CH_4 (2nd panel, Fig. 4), C_2H_4 (2nd panel, Fig. 5), C_6H_6 (6th panel, Fig. 5) emissions, which are very noisy.

Using ground-based observational data over a 10 year period, Caldwell et al. (1988) found that the 8 μm CH_4 emission remains around 180° longitude on 60° N latitude, whereas during the same period the southern CH_4 emission moves around in longitude near 60o S latitude. Our CH_4 emission results in this work are consistent with those of Caldwell et al. The Voyager 2 C_2H_4 emissions (2nd panel, Fig. 5) and Voyager 2 C_6H_6 emissions (6th panel, Fig. 5) are very noisy and do not contain meaningful longitudinal information.

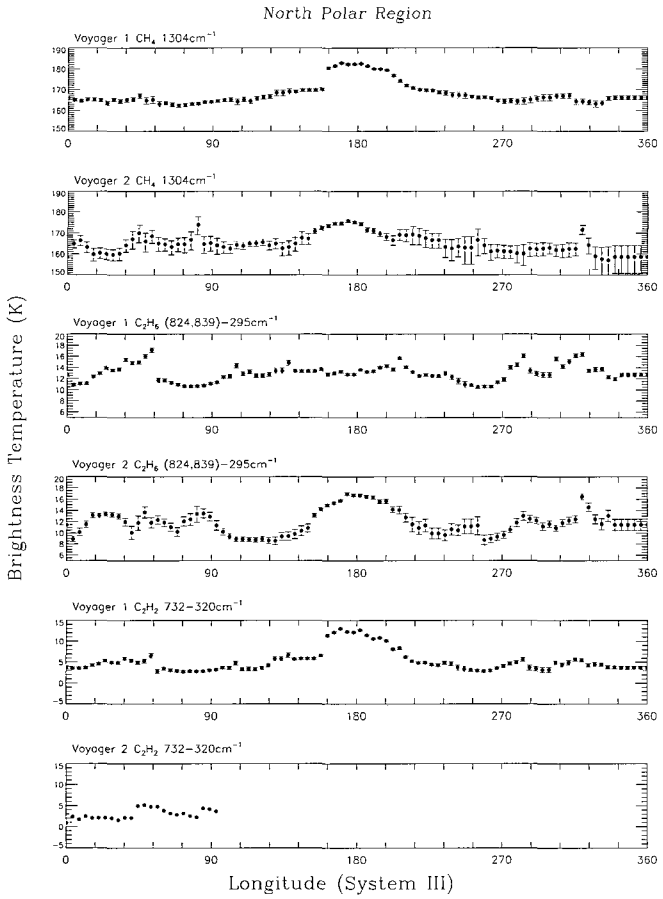

Fig. 2.— Comparisons between north polar Voyager 1 and 2 data for CH_4, C_2H_6, and C_2H_2 emissions. Enhanced emissions in the CH_4, and C_2H_2 bands are clearly seen in both Voyager data between 160° and 200° longitude. $\pm 1\sigma$ error bars are presented in Figs. 2 through 5. The negative values in Fig. 2 through 5 result from the subtractions of the adjacent continua.

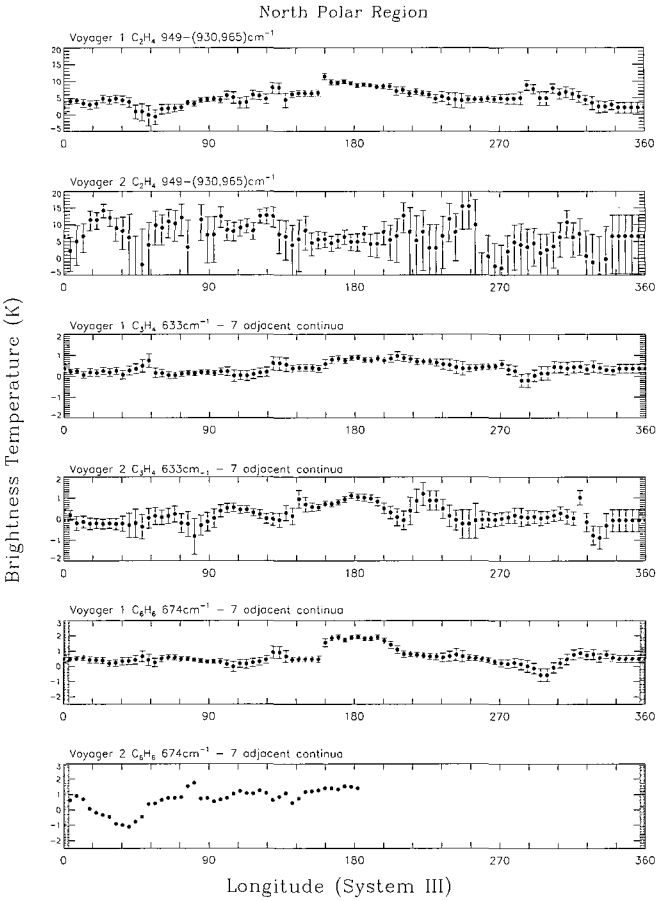

Fig. 3.— Comparisons between north polar Voyager 1 and 2 data for C_2H_4, C_3H_4, and C_6H_6 band emissions. Detailed longitudinal variations for the band emissions of these hydrocarbons are exhibited. In Figs. 2, 3, 4, and 5, in addition to the auroral emissions, we can see apparent longitudinal stratospheric structures, which are discussed in Section 4.

IV. STRATOSPHERIC WAVE FEATURES

Magalhães et al. (1989) discovered tropospheric large scale features, which move slowly, using Voyager IRIS data at 45 μm. Deming et al. (1989) also detected similar tropospheric thermal wave structures in 8 - 13 μm images obtained at the NASA Infrared Telescope Facility (IRTF). They found a zonal wavenumber of $\sim$11 at 20° north, which were unchanged over two Jovian rotations. On the other hand, stratospheric wave-like structures were seen in infrared images obtained at the IRTF with a wide band filter centered on the strong CH_4 band at 7.8 μm (Orton et al. 1991). Orton et al. suggested that the stratospheric waves originate as instabilities in the troposphere and propagate vertically upward, increasing their amplitude along the way as the background atmospheric density decreases with altitude.

During the Cassini swing-by of Jupiter in December 2000, the CIRS obtained infrared spectra of Jupiter in the 7.14 $\sim$ 16.67 μm range with a spectral resolution of 0.003 μm and spatial resolutions of approximately 3° covering the entire globe (e.g., Flasar et al. 2001; Achterberg et al. 2001). Using these spectra, they were able to construct tropospheric and stratospheric images, which reveal wave-like features. Achterberg et al. (2001) found that the images are dominated by zonal wavenumber 2 with wavenumbers 1 through 4 at various pressure ranges and several latitudes. They found that significant waves are seen at wavenumber 10 near the equator at 10 mbar, and with wavenumber 14 around 15° N and 214 mbar. Harrington et al. (2001) observed Jupiter at the NASA/IRTF with the MIRLIN camera, and reported stratospheric waves with zonal wavenumber 1 and 13 at 18° S.

In Figures 6 and 7, we present our Jupiter images (or brightness temperature maps) of Voyager 1 and 2, respectively, for the CH_4, C_2H_2, and C_2H_6 band emissions, which were binned with a 20° $\times$ 20° box, as de-

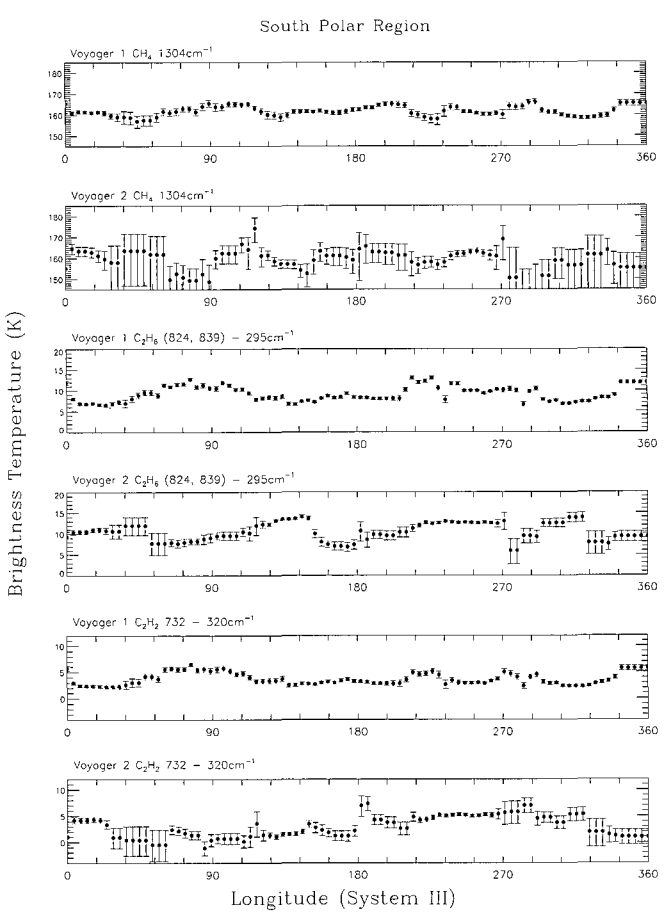

Fig. 4.— Comparisons between south polar Voyager 1 and 2 data for CH_4, C_2H_6, and C_2H_2 emissions.

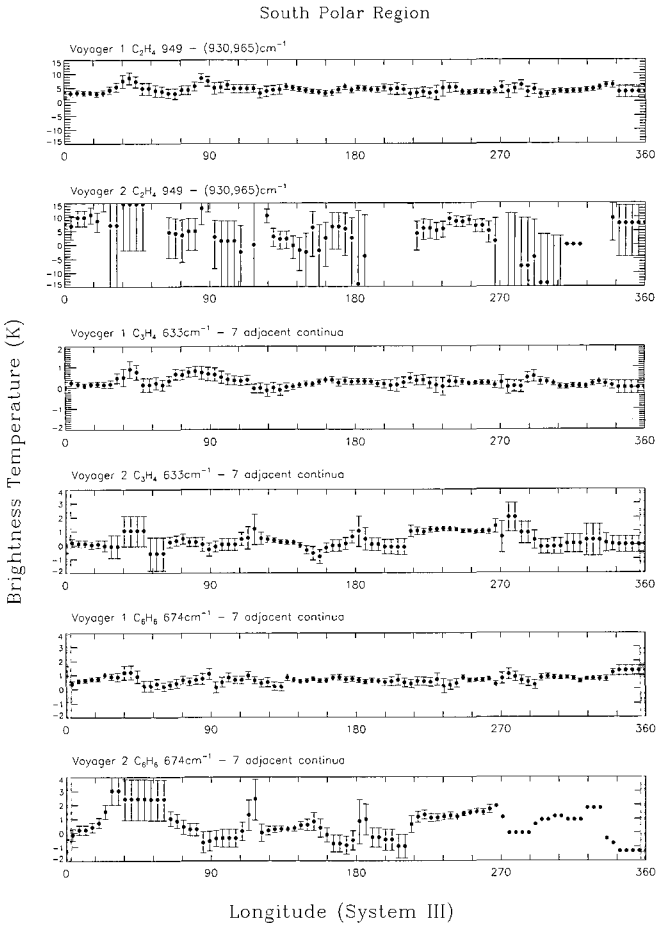

Fig. 5.— Comparisons between south polar Voyager 1 and 2 data for C_2H_4, C_3H_4, and C_6H_6 emissions.

scribed in Section 2. We did not present similar images for minor hydrocarbons because the S/N ratios of these images are too low to be presented. The stratospheric patterns in IRIS 7.8 μm CH_4 images could not be seen previously because the IRIS images without using a large bin are too noisy for discerning the infrared features.

In Figure 8, we present binned images for stratospheric C_2H_2 and C_2H_6 emissions for 2 - 3 days before the closest Voyager 1 encounter with Jupiter. The tropospheric image at the top of Figure 8 was taken at 31.25 μm, where the tropospheric PIA of H_2 is dominant. The Great Red Spot (GRS) can be clearly seen around 70° longitude in the southern hemisphere, and other smaller features can also be seen in this tropospheric image. However, the GRS is not apparent in other stratospheric images in Figures 6, 7, and 8. In these images, apparent wave-like features, which are definitely above the noise levels, are seen in addition to the prominent north polar brightenings. Comparing the stratospheric features in Figure 8 (for 2 - 3 days before the closest Voyager 1 encounter with Jupiter), and those in Figure 6 (which are averaged images for the 12 days of the Voyager 1 encounter), we found that the some of major stratospheric features are not significantly changes, but other features are changed in brightness and/or location, indicating the degree of stability of the stratospheric features during the 12 days of the encounter. A preliminary result was previously reported by Kim et al. (1996).

Fourier transform analyses applied to these images yield wavenumbers 5 - 7 between 10° and 45° N and 10° and 40° S latitudes for the C_2H_2 image in Figure 6; and wavenumber ~6 between 10° and 45° N latitudes and wavenumber ~7 between 10° and 40° S latitudes for the C_2H_2 image in Figure 8. Between 10° S and 10° N latitudes (the equatorial region) there seem to no dominant wavenumbers in the power spectra of these images. Fourier transform analyses of CH_4 and C_2H_6 images, although they are noisier than C_2H_2 images, yield similar wavenumbers, i.e., 5 - 7. In the tropospheric image in Figure 8, we found wavenumbers of 5 - 7 for the same latitudinal regions, and these wavenumbers are different from those found by Magalhães et al. (1989) and Deming et al. (1989). Our stratospheric wavenumbers are also different from the recent values resulted

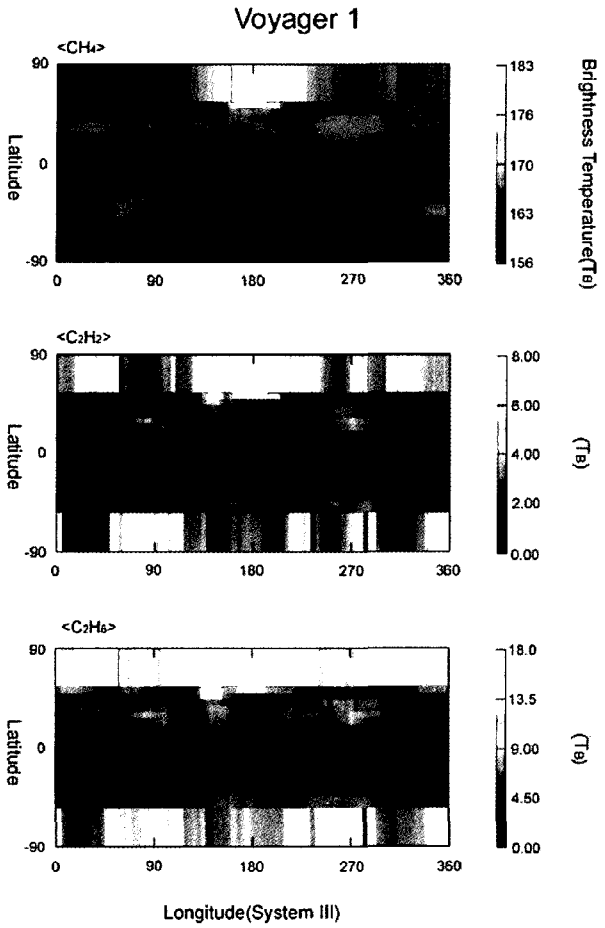

Fig. 6.— Jupiter images, the maps of brightness temperatures, of the CH_4, C_2H_2, and C_2H_6 emissions obtained from Voyager 1 IRIS spectral data.

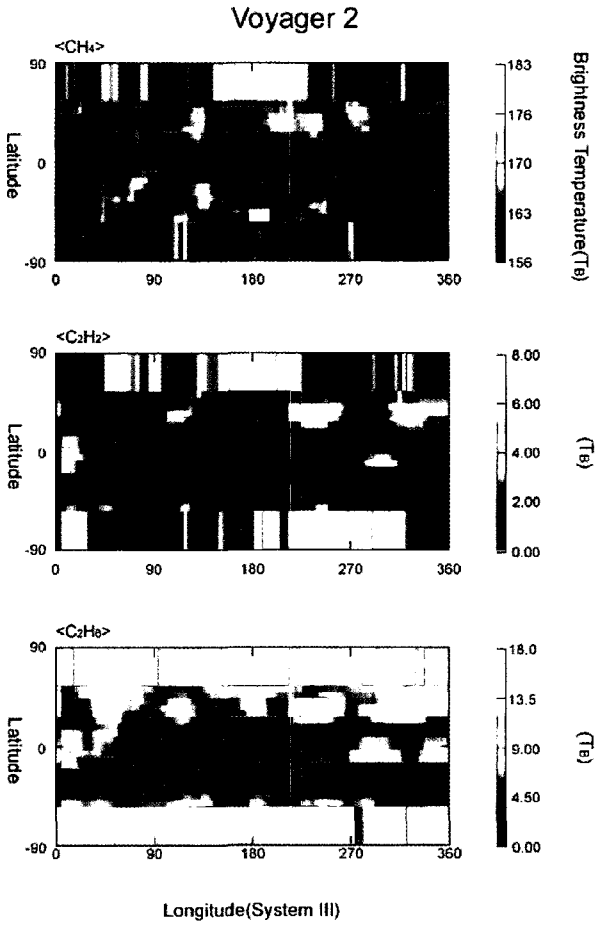

Fig. 7.— Jupiter images of the CH_4, C_2H_2, and C_2H_6 emissions obtained from Voyager 2 IRIS data.

from the CIRS and ground-based observations by various authors (e.g., Flasar et al. 2001; Achterberg et al. 2001; Harrington et al. 2001).

V. DISCUSSION

In principle, stratospheric temperatures can be retrieved from the 7.8 μm CH_4 line-by-line intensities, and then abundances of other hydrocarbons should be derived utilizing the derived stratospheric temperatures and the hydrocarbon emission intensities. Ideally, therefore, the CH_4 intensity map can be transformed into a stratospheric temperature map, and in turn the hydrocarbon intensity maps can be transformed into abundance maps of the hydrocarbons. There are, however, two obstacles to carry out this task: (1) too noisy intensity maps (especially for C_2H_4, C_3H_4, and C_6H_6 bands) for this purpose; and (2) the difficulty in separating temperature increases from hydrocarbon abundance enhancements in the auroral regions – A study on thermal profiles in the auroral regions of Jupiter (Drossart et al. 1993), and another studies on high temperatures in the thermosphere of Jupiter (Kim et al. 1990; Maillard et al. 1990) indicate that the observed excess hydrocarbon emission bands can be explained by high temperatures in the low thermosphere (or in the upper stratosphere) without increasing hydrocarbon abundances compared with those in the other regions of Jupiter. In other word, the enhanced hydrocarbon emission simply cannot be translated into abundance increase. It is also difficult to constrain temperatures in the upper stratosphere (or in the lower thermosphere) using only the Voyager CH_4 emission. Therefore, in this paper, we do not present the stratospheric temperature maps and hydrocarbon abundance maps.

Recent Cassini CIRS (e.g., Flasar et al. 2001; Achterberg et al. 2001) and NASA/IRTF (Harrington

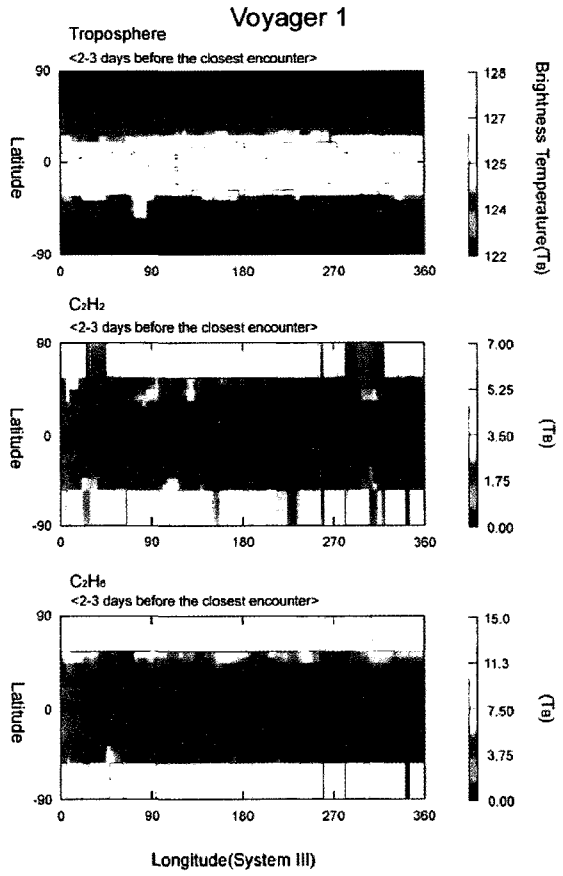

Fig. 8.— Tropospheric image (top) of Jupiter at 31.25 μm, stratospheric image (middle) of C_2H_2, stratospheric image (bottom) of C_2H_6 taken by Voyager 1 IRIS during 2 - 3 days before the closest encounter with Jupiter.

et al. 2001) results yield various wavenumbers from 1 to 13 for the stratospheric waves. These wavenumbers are different from our values derived from the Voyager IRIS images, and are also different from those derived from tropospheric features by Magalhães et al. (1989) and Deming et al. (1989). The differences in the wavenumber among these observations suggest that the stratospheric circulation (e.g., Conrath et al. 1990) and tropospheric dynamics significantly influence the pattern of the wave-like features as a function of time. Thus far, the inconsistency among the derived wavenumbers has not been explained. However, as we have shown a time-variability in the IRIS spectra within the 4 month period between the two Voyager encounters, one strong possibility is that the wavenumber is time-variable. Other possibility is that the observational data may not be enough to establish the Jovian wavenumber. Further observations from space and ground, and further theoretical considerations are needed to establish the nature of time variability of the wave-like features.

VI. CONCLUSIONS

The Voyager 1 and 2 IRIS data for the north polar region of Jupiter show enhanced emissions in CH_4 and C_2H_2 bands between 160° and 200° N longitude. Enhanced C_2H_6 emission in the northern hot spot is not obvious in the Voyager 1 data, but it is quite prominent in the Voyager 2 data indicating significant intensity variation within the 4 month period between the two Voyager encounters. Voyager 1 data show definite enhancement of C_2H_4 emission between 160° - 200° N longitude. Voyager 1 north polar C_2H_4 and C_3H_4 emissions may be wider (i.e., 140° - 240° longitude) than Voyager 2 C_3H_4 and Voyager 1, 2 C_6H_6 emissions, which are approximately confined between 160° and 200° longitude. Voyager 1 south polar data show C_2H_6 and C_2H_2 emission enhancements between 50° and 110°, but no similar enhancement for other Voyager 1 hydrocarbon emissions. Voyager 2 south polar data between 190° and 270° longitude show an emission enhancement for the C_2H_2 band.

The Voyager IRIS stratospheric images also reveal patterns of stratospheric waves, which are similar to those seen from previous ground-based and space-borne observations, but differ in wavenumbers. Fourier transform analyses of these images yield wavenumbers 5 - 7 at mid-Northern and mid-Southern latitudes, which are different from those resulted from recent Cassini CIRS and previous ground-based observations. The different wavenumbers obtained at the different observations suggest a time variability of the wave-like features.

ACKNOWLEDGEMENTS

SJK and HJS have been supported by a grant (R14-2002-043-01003-0) from the Korea Research Foundation. WC was supported by the KOSEF (R01-2003-000-10131-0) and the BK21 program. We thanks Drs. T.A. Livengood, P.N. Romani, and R.N. Halthore for providing valuable discussions during the early stage of this research.

REFERENCES

Achterberg, R. K., Conrath, B.J., Flasar, F.M., Simon-Miller, A.A., Nixon, C. A., & Bezard, B., 2001, Cassini CIRS Observations of Thermal Waves on Jupiter, BAAS, 33, 1035

Allison, M., 1990, Planetary waves in Jupiter's equatorial atmosphere, Icarus, 83, 282

Bezard, B., Encrenaz, T., Lellouch, E., & Feuchtgruber, H., 1999, A New Look at the Jovian Planets, Science, 283, 800

Caldwell, J., Gillett, F. C., & Tokunaga, A. T., 1980, Possible infrared aurorae on Jupiter, Icarus, 44, 667

Caldwell, J., Tokunaga, A. T., & Orton G., 1983, Observational constraints on the atmospheres of Uranus and

Neptune from new measurements near 10 micrometers, Icarus 53, 133

Caldwell, J., Halthore, R., Orton, G., & Bergstralh, J., 1988, Infrared polar brightenings on Jupiter. IV - Spatial properties of methane emission, Icarus 74, 331

Conrath, B. J., & Gautier, D. 1980. In Interpretation of Remote Sensing of Atmospheres and Oceans (A. Deepak, Ed.), pp. 611-630. Academic Press, New York.

Conrath, B. J., Gierasch, P.J., & Leroy, S.S., 1990, Temperature and circulation in the stratosphere of the outer planets, Icarus, 83, 255.

Deming, D., Mumma, M.J., Espenak, F., Jennings, D.E., Kostiuk, T., Wiedemann, G., Loewenstein, R., & Piscitelli, J., 1989, A search for p-mode oscillations of Jupiter - Serendipitous observations of nonacoustic thermal wave structure, ApJ, 343, 456

Drossart, P., Bezard, B., Atreya, S. K., Bishop, J., Waite, J.H., & Boice, D. J., Thermal profiles in the auroral regions of Jupiter, 1993 JGR, 98, 18803

Fisher, B. M., & Orton, G. S., 2000, Jupiter's Tropospheric Temperature Structure in 1996 and 1997, BAAS, 32, 1015

Flasar, F. M., Simon-Miller, A. A., Achterberg, Conrath, B. J., Gierasch, P. J., Kunde, V. G., Nixon, C., Jennings, D. E., Romani, P. N., Irwin, P., Bezard, B., Carlson, R., & Cassini CIRS team, 2001, Prospecting Jupiter in the Thermal Infrared with Cassini CIRS: Atmospheric Temperatures and Dynamics, BAAS, 33, 1025.

Gierasch, P. J., Conrath, B. J. & Magalhães, J. A., 1986, Zonal mean properties of Jupiter's upper troposphere from Voyager infrared observations, Icarus 67, 456

Hanel, R. et al. 1979a, Infrared observations of the Jovian system from Voyager 1, Science, 204, 972

Hanel, R. et al. 1979b, Infrared observations of the Jovian system from Voyager 2, Science, 206, 952

Hanel, R. A., Herath, L. W., Kunde, V. G., & Pearl, J.C. 1980, NASA Rept. X-693-821-8.

Harrington, J., Deming, D., Ruane, A., & Vatanavigkit, S., 2001, Jupiter's Short-Term Tropospheric and Stratospheric Thermal Dynamics Before and During the Cassini Encounter, BAAS, 33, 1025

Kim, S., Caldwell, J., Rivolo, R., Wagener, R. & Orton, G., 1985, Infrared polar brightening on Jupiter. III - Spectrometry from the Voyager 1 IRIS experiment, Icarus, 64, 233

Kim, S. J., Drossart, P., Caldwell, J., & Maillar, J.-P. 1990, Temperatures of the Jovian auroral zone inferred from 2-micron H_2 quadrupole line observations, Icarus, 84, 54

Kim, S. J., Bjoraker, G., Kostiuk, T., Livengood, T., & Romani, P., 1996, Stratospheric Images of Jupiter Derived from Hydrocarbon Emissions in Voyager 1 and 2 IRIS Spectra, BAAS, 28, 1147

Kunde, V., Hanel, R., Maguire, W. Gautier, D., Baluteau, J. P., Martin, A., Chedin, A., Husson, N., & Scott, N. 1982, The tropospheric gas composition of Jupiter's north equatorial belt /NH3, PH3, CH3D, GeH4, H2O/ and the Jovian D/H isotopic ratio, ApJ, 263, 443

Magalhães, J. A., Weir, A. L., Gierasch, P. J., Conrath, B. J. & Leroy, S. S., 1990, Zonal motion and structure in Jupiter's upper troposphere from Voyager infrared and imaging observations, Icarus, 88, 39

MMagalhães, J. A., Weir, A.L., Conrath, B.J., Gierasch, P. J. & Leroy, S. S., 1989, Slowly moving thermal features on Jupiter, Nature. 337, 44

Maillard, J.-P., Drossart, P., Watson, J. K. G., Kim, S. J. & Caldwell, J., 1990, H3(+) fundamental band in Jupiter's auroral zones at high resolution from 2400 to 2900 inverse centimeters, ApJ, 363, L37

Marten, A., Rouan, D., Baluteau, J. P., Gautier, D., Conrath, B. J., Hanel, R. A., Kunde, V., Samuelson, R., Chedin, A., & Scott, N., 1981, Study of the ammonia ice cloud layer in the Equatorial Region of Jupiter from the infrared interferometric experiment on Voyager, Icarus 46, 233

Orton, G. S. Friedson, A. J., Caldwell, J., Hammel, H. B., Baines, K. H., Bergstralh, J. T., Martin, T. Z., Malcom, M. E., West, R. A., Golisch, W. F., Griep, D. M., Kaminski, C.D., Tokunaga, A. T., Baron, R., & Shure, M., 1991, Middle infrared thermal maps of Venus at the time of the Galileo encounter, Science 252, 537

Sanchez-Lavega, A., Hueso, R., & Acarreta, J. R., 1998, A System of Circumpolar Waves in Jupiter's Stratosphere BAAS, 30, 1068